

Direct and instantaneous observation of intravenously injected substances using intravital confocal micro-videography

Yu Matsumoto,^{1,2,3} Takahiro Nomoto,⁴ Horacio Cabral,⁴ Yoko Matsumoto,⁵
Sumiyo Watanabe,^{1,6,7} R. James Christie,⁸ Kanjiro Miyata,¹ Makoto Oba,⁹
Tadayoshi Ogura,¹⁰ Yuichi Yamasaki,⁸ Nobuhiro Nishiyama,¹ Tatsuya Yamasoba,²
and Kazunori Kataoka^{1,4,8,*}

¹*Division of Clinical Biotechnology, Center for Disease Biology and Integrative Medicine, Graduate School of Medicine, The University of Tokyo, Japan*

²*Department of Otorhinolaryngology and Head and Neck Surgery, Graduate School of Medicine and Faculty of Medicine, The University of Tokyo, Japan*

³*Department of Otorhinolaryngology and Head and Neck Surgery, Mitsui Memorial Hospital, Japan*

⁴*Department of Bioengineering, Graduate School of Engineering, The University of Tokyo, Japan*

⁵*Department of Obstetrics and Gynecology, Graduate School of Medicine and Faculty of Medicine, The University of Tokyo, Japan*

⁶*Division of Nephrology and Endocrinology, Department of Internal Medicine, Graduate School of Medicine and Faculty of Medicine, The University of Tokyo, Japan*

⁷*Department of Internal Medicine, Teikyo University School of Medicine, Japan*

⁸*Department of Materials Engineering, Graduate School of Engineering, The University of Tokyo, Japan*

⁹*Department of Vascular Regeneration, Division of Tissue Engineering, The University of Tokyo Hospital, Japan*

¹⁰*Nikon Instech Co., Ltd., Japan*

*kataoka@bmw.t.u-tokyo.ac.jp

Abstract: We describe the development and application of intravital confocal micro-videography to visualize entrance, distribution, and clearance of drugs within various tissues and organs. We use a Nikon A1R confocal laser scanning microscope system attached to an upright ECLIPSE FN1. The Nikon A1R allows simultaneous four channel acquisition and speed of 30 frames per second while maintaining high resolution of 512×512 scanned points. The key techniques of our intravital imaging are (1) to present a flat and perpendicular surface to the objective lens, and (2) to expose the subject with little or no bleeding to facilitate optical access to multiple tissues and organs, and (3) to isolate the subject from the body movement without compressing the blood vessels, and (4) to insert a tail vein catheter for timed injection without moving the subject. Ear lobe dermis tissue was accessible without surgery. Liver, kidney, and subcutaneous tumor were accessed following exteriorization through skin incision. In order to image initial extravasations of compounds into tissue following intravenous injection, movie acquisition was initialized prior to drug administration. Our technique can serve as a powerful tool for investigating biological mechanisms and functions of intravenously injected drugs, with both spatial and temporal resolution.

© 2010 Optical Society of America

OCIS codes: (170.1790) Confocal microscopy; (170.2655) Functional monitoring and imaging.

References and links

1. I. Veilleux, J. A. Spencer, D. P. Biss, D. Cote, and C. P. Lin, "In Vivo Cell Tracking With Video Rate Multimodality Laser Scanning Microscopy," *IEEE J. Sel. Top. Quantum Electron.* **14**(1), 10–18 (2008).
2. P. Kim, M. Puoris'haag, D. Côté, C. P. Lin, and S. H. Yun, "In vivo confocal and multiphoton microendoscopy," *J. Biomed. Opt.* **13**(1), 010501 (2008).
3. P. Kim, E. Chung, H. Yamashita, K. E. Hung, A. Mizoguchi, R. Kucherlapati, D. Fukumura, R. K. Jain, and S. H. Yun, "In vivo wide-area cellular imaging by side-view endomicroscopy," *Nat. Methods* **7**(4), 303–305 (2010).
4. R. Mehvar, M. A. Robinson, and J. M. Reynolds, "Molecular weight dependent tissue accumulation of dextrans: in vivo studies in rats," *J. Pharm. Sci.* **83**(10), 1495–1499 (1994).

5. R. Mehvar, and T. L. Shepard, "Molecular-weight-dependent pharmacokinetics of fluorescein-labeled dextrans in rats," *J. Pharm. Sci.* **81**(9), 908–912 (1992).
6. G. Zhang, V. Budker, and J. A. Wolff, "High levels of foreign gene expression in hepatocytes after tail vein injections of naked plasmid DNA," *Hum. Gene Ther.* **10**(10), 1735–1737 (1999).
7. F. Liu, Y. Song, and D. Liu, "Hydrodynamics-based transfection in animals by systemic administration of plasmid DNA," *Gene Ther.* **6**(7), 1258–1266 (1999).
8. H. Herweijer, and J. A. Wolff, "Progress and prospects: naked DNA gene transfer and therapy," *Gene Ther.* **10**(6), 453–458 (2003).
9. D. Liu, and J. E. Knapp, "Hydrodynamics-based gene delivery," *Curr. Opin. Mol. Ther.* **3**(2), 192–197 (2001).
10. A. Crespo, A. Peydró, F. Dasí, M. Benet, J. J. Calvete, F. Revert, and S. F. Aliño, "Hydrodynamic liver gene transfer mechanism involves transient sinusoidal blood stasis and massive hepatocyte endocytic vesicles," *Gene Ther.* **12**(11), 927–935 (2005).
11. T. Suda, X. Gao, D. B. Stolz, and D. Liu, "Structural impact of hydrodynamic injection on mouse liver," *Gene Ther.* **14**(2), 129–137 (2007).
12. G. Zhang, X. Gao, Y. K. Song, R. Vollmer, D. B. Stolz, J. Z. Gasiorowski, D. A. Dean, and D. Liu, "Hydroporation as the mechanism of hydrodynamic delivery," *Gene Ther.* **11**(8), 675–682 (2004).
13. Y. Ohno, H. Birn, and E. I. Christensen, "In vivo confocal laser scanning microscopy and micropuncture in intact rat," *Nephron, Exp. Nephrol.* **99**(1), e17–e25 (2005).

Introduction

In vivo imaging has received much attention in recent years, as it can elucidate the complex biological and pathological events within a living animal. Although histological examination of excised tissues has long served as a fundamental approach for tissue analysis, intravital confocal microscopy provides instant histopathology at the cellular and subcellular level and therefore is ideal for investigating dynamic events involved. Here we describe the development and application of intravital confocal micro-videography to visualize entrance, distribution, and clearance of drugs within various tissues and organs. In order to image initial extravasations of compounds into tissue following intravenous injection, movie acquisition was initialized prior to drug administration. Many groups have adapted commercial confocal microscopes for intravital imaging, but they often use conventional galvano scanners with slow acquisition speed. Progressive groups build confocal and/or multi-photon microscopes and even microendoscopes with rapid scanning systems in-house to achieve video-rate imaging [1–3].

Table 1. Commercially available rapid scanning confocal microscopes

Vendor	Product Name	Scanning System	Maximum Frame Rate at 512 x 512 Pixels	Number of Simultaneously Detectable Channels
Nikon	A1R	Resonant Scanner	30 fps	4
Leica	TCS SP5 II	Resonant Scanner	25 fps	5
Microsystems	LSM 7 LIVE	Linear Scanner	120 fps	2
Carl Zeiss	LSM 7 LIVE	Linear Scanner	120 fps	2
Yokogawa Electric	CSU-X1	Nipkow spinning disk	2000 fps	3
Olympus	DSU	Spinning Disk Confocal	15 fps	1

Recently, several rapid scanning confocal microscopes became commercially available (Table 1). Although all vendors primarily recommend use of their products with an inverted configuration (optimized for live cell imaging), combination with an upright microscope has advantages for intravital imaging. Here, we attached a Nikon A1R confocal laser scanning microscope system to an upright ECLIPSE FN1 to acquire video images. The A1R incorporates both a conventional galvano scanner and also a high-speed resonant scanner, which allows an acquisition speed of 30 frames per second and simultaneous four channel detection, while maintaining high resolution of 512×512 scanned points. Our technique consists of the following essential features:

- (1) Front-end design presenting a flat and perpendicular surface against the objective lens;

- (2) Exposure surgery with little or no bleeding to facilitate optical access to multiple tissues and organs;
- (3) Stabilization of the sample to isolate from the body movement without compressing the blood vessels;
- (4) Tail vein catheterization for timed injection during data acquisition, without moving the subject;

Our technique is particularly effective for investigating the dynamic and complex events that occur immediately following drug administration. We investigated the influence of molecular weight on pharmacokinetic behavior by imaging the ear lobe dermis. We also investigated the accumulation of pDNA within liver tissue by hydrodynamic injection. Kidney and tumor tissues were imaged to observe renal excretion and tumor extravasation.

Results and discussion

During the development of a promising drug delivery system, there is a strong need to accurately grasp the intravital behavior of the administered drugs [4,5]. We investigated the influence of molecular weight on pharmacokinetic behavior using fluorescein (MW = 332) and fluorescein-labeled dextrans (FD) with average molecular weights of 10-, 40-, and 500 kDa (Fig. 1). Fluorescein and FDs demonstrated different pharmacokinetics [Fig. 1(c), 1(e), [Media 1](#), [Media 2](#), [Media 3](#), and [Media 4](#)]. Arterial entrance was observed 10 seconds after injection, followed by venous migration 30 seconds after injection. Fluorescein diffused into extravascular tissue concurrently with venous migration. FD 10 kDa gradually translocated into extravasculature tissue 10-15 minutes after injection and lymphatic drainage was observed after 20 minutes. FD 70- and 500 kDa remained in the vasculature during the entire 60-minute observation period. Our confocal micro-videography technique is superior to conventional methods used to study plasma clearance in regard to the number of animals needed to generate a clearance curve and also the ability to obtain more information from a single experiment. Conventional protocols used in plasma clearance studies require blood extraction at various post-injection time points, using multiple animals. In contrast, intravital confocal micro-videography yields 30 time points per seconds before, during, and after the injection. Moreover, our technique provides spatial resolution so that we can individually investigate multiple regions such as arteries, veins, extravascular tissue, lymphatic vessels, and even cells and nuclei if desirable [Fig. 1(d)]. For long-term plasma clearance studies, however, we still perform conventional methods in conjunction with our technique because prolonged anesthesia periods longer than five hours are not practical.

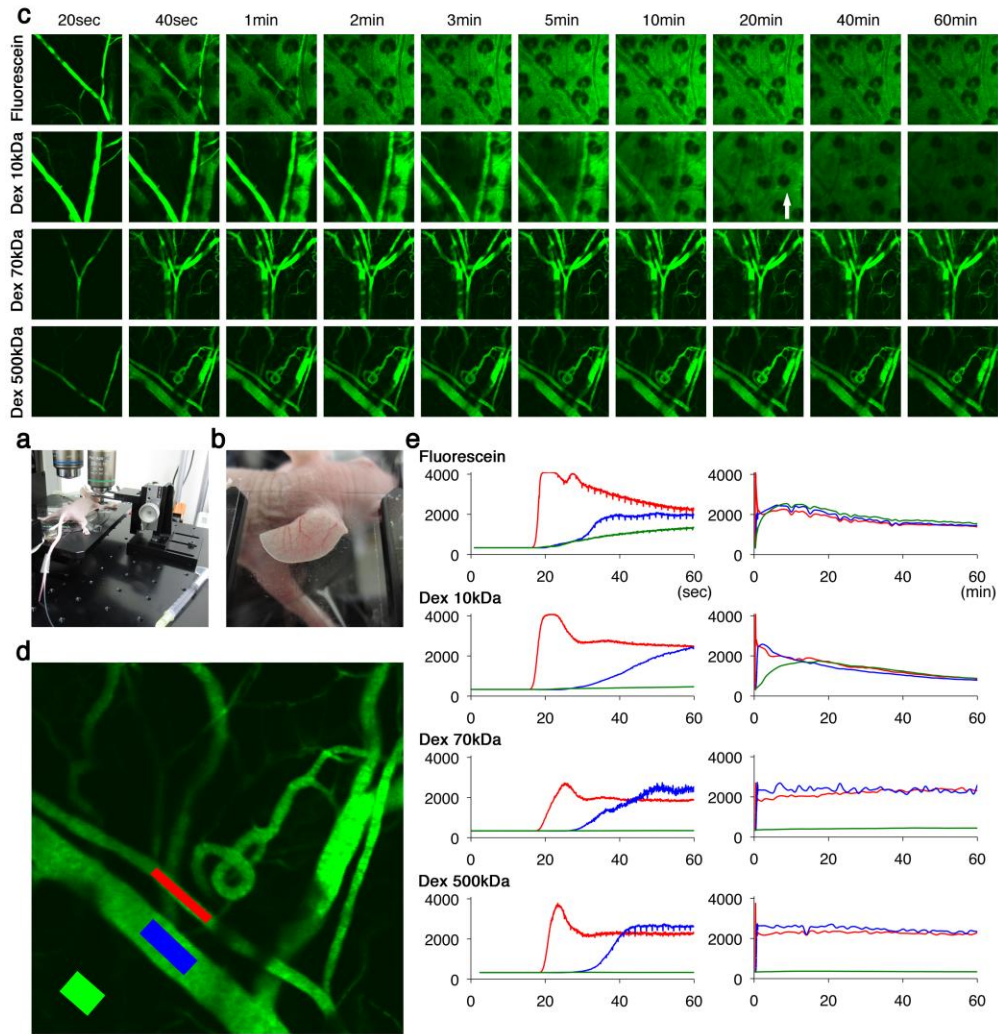


Fig. 1. (a) The earlobe is an excellent location for intravital confocal micro-videography because blood vessels are easily observed in the dermis and the ear is easily accessed and positioned in the imaging apparatus. (b) Earlobe was attached to the coverslip with a small drop of immersion oil. (c) Fluorescein, FD 10-, 70-, and 500 kDa were administered via tail vein catheter 10 seconds after movie acquisition was initiated. Video-rate (30 fps) movies were recorded for the first minute, and subsequent time-lapse images were recorded every minute for an additional 60 minutes. The arrow indicates lymphatic drainage. Obtained data sets were further processed using Nikon NIS-Elements C software. Image size: $645.50\mu\text{m} \times 645.50\mu\text{m}$. (d) Three regions of interest (ROI) are selected respectively as an artery (red), vein (blue), and extravascular skin tissue (green). Image size: $645.50\mu\text{m} \times 645.50\mu\text{m}$. (e) Fluorescence intensity in these ROIs plotted against time. All movies are provided as supplementary movie files ([Media 1](#), [Media 2](#), [Media 3](#), and [Media 4](#)).

The liver is a vital organ that has a wide range of functions, including detoxification, protein synthesis, storage, and production of bile. Real-time imaging of liver dynamics and small changes in hepatocytes will provide insight to poorly understood processes that occur in the liver. We applied our real-time imaging technique to observe the accumulation of pDNA within liver tissue by hydrodynamic injection [Fig. 2(a)]. Delivery of pDNA by hydrodynamic injection involves rapid tail vein injection of a large volume of pDNA solution and efficient accumulation of pDNA in the liver is reported [6,7]. This method has been widely utilized by the gene therapy community for evaluating therapeutic activities of various genes [8,9].

Following normal injection, pDNA flowed into the hepatic lobule from the hepatic artery, through the sinusoids, and towards the central vein (Media 5). After 20 minutes, pDNA was observed adjacent to vessel walls, but was rarely transferred into hepatic cells. In contrast, hydrodynamic injection of pDNA resulted in initial flow into the hepatic lobule from the hepatic artery, but the flow stopped at the sinusoids. After 50 seconds, pDNA appeared from the central vein, indicating retrodynamic blood flow. Blood flow oscillated back and forth within the sinusoids, indicating that the blood pressure of central and portal vein remained in equilibrium, which lasted as long as 3 minutes (Media 6). During the 30-minute period after injection, pDNA was observed in more hepatic cell nuclei by hydrodynamic injection than normal injection. It has been hypothesized that hydrodynamic injection generates retrodynamic blood flow from the central vein [10–12]. This hypothesis was well described by performing dual pressure detector system of the portal vein and inferior vena cava, and is further supported by our results obtained by direct imaging of the hepatic lobule.

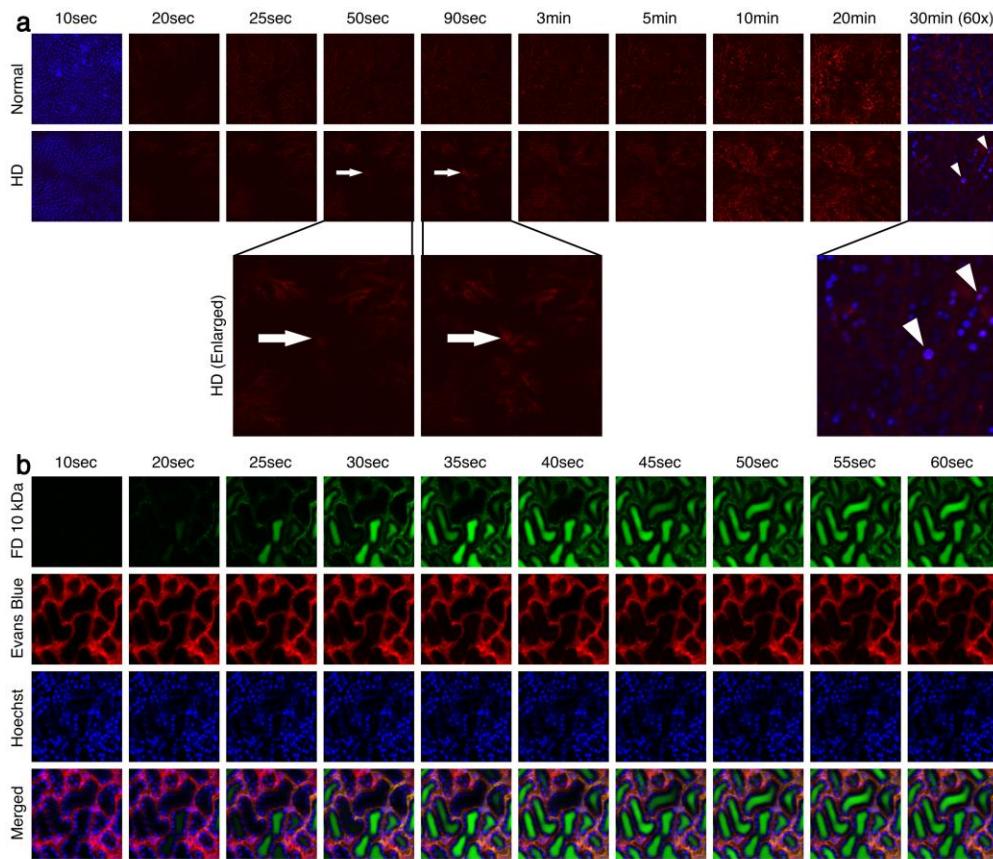


Fig. 2. (a) Intravital confocal micro-videography of the mouse hepatic lobule. Hoechst (blue) was intravenously injected 15 minutes before imaging. Cy5-labeled pDNA (red) were normally or hydrodynamically (HD) injected via tail vein catheter 10 seconds after movie acquisition was initiated (Media 5 and Media 6). Image frames were extracted from both videos at identical time points for comparison. Image size: $645.50\mu\text{m} \times 645.50\mu\text{m}$. Zoomed pictures were taken 30 minutes after injection. Image size: $212.13\mu\text{m} \times 212.13\mu\text{m}$. Hoechst channels are shown at 10 sec and 30 min for histological comprehension. Arrows indicate reverse blood flow from central vein. Arrowheads indicate nuclei that pDNA were successfully transferred. (b) Intravital confocal micro-videography of mouse kidney tissue. Hoechst (blue) and Evan's Blue dye (red) were intravenously injected 15 minutes and 5 minutes before imaging, respectively. FD 10 kDa (green) were administered via tail vein catheter 10 seconds after movie acquisition was initiated (Media 7). Image size: $645.50\mu\text{m} \times 645.50\mu\text{m}$.

To further demonstrate the feasibility of our technique, kidney and tumor tissues were imaged to observe renal excretion and tumor extravasation. Deeper kidney structures such as glomeruli could not be imaged because renal tissue highly absorbs and scatters light [13]. Although the imaging of the renal cortex was limited to shallow features such as proximal and distal tubules and capillary vessels, we still could evaluate glomerular filtration indirectly [Fig. 2(b)]. FD 10 kDa flowed into the capillary blood vessels and proximal tubules at the same time, which indicate that FD 10 kDa were immediately filtered by glomerulus. FD 10 kDa flowed into the distal tubules shortly afterward, until all the tubules were filled. The albumin - Evan's blue dye complex remained in blood circulation throughout the study for 60 minutes. Observation of the albumin - Evan's blue dye complex also depicted tumor vasculature [Fig. 3(a)]. Multiple frames were merged to produce a wide-area image [Fig. 3(b)].

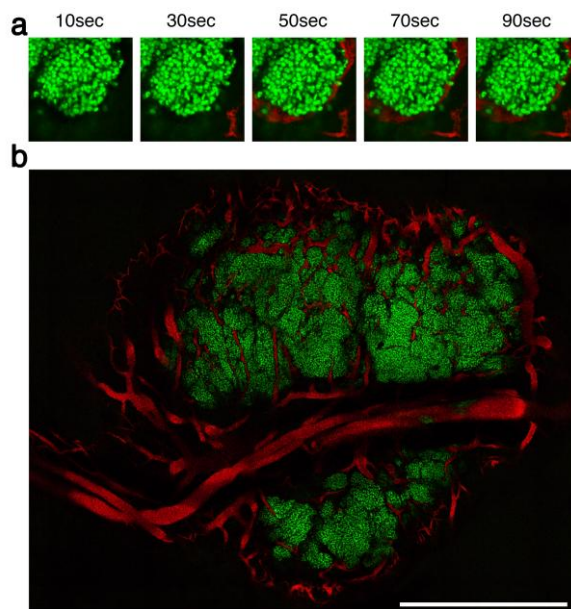


Fig. 3. (a) Intravital confocal micro-videography of subcutaneous HeLa-H2BGFP tumor. Evan's blue dye was administered via tail vein catheter 10 seconds after movie acquisition was initiated. Image frames were extracted from the video at indicated time points. Image size: $212.13\mu\text{m} \times 212.13\mu\text{m}$ (b) Motorized XY stage enables 'large image acquisition' feature of the Nikon NIS-Elements C software. Multiple frames were automatically captured in sequence and merged to produce a wide-area image. Scale bar: 1 mm.

Arterial entrance, venous migration, extravasation into tissue, and clearance was directly observed within various tissues and organs. The intravital confocal micro-videography technique described here is useful for investigating biological mechanisms and functions in both spatial and temporal resolution. Our technique is particularly effective for investigating the dynamic and complex events that occur immediately following drug administration, such as first path effects, site-specific drug accumulation, blood circulation and metabolism behavior.

Materials and methods

Microscope

All picture/movie acquisitions were performed using a Nikon A1R confocal laser scanning microscope system attached to an upright ECLIPSE FN1 (Nikon Corp., Tokyo, Japan). The A1R incorporates both conventional a galvano scanner and also a high-speed resonant scanner. The resonant scanner allows an acquisition speed of 30 frames per second while

maintaining high resolution of 512×512 scanned points. Modification of the ECLIPSE FN1 was necessary for intravital imaging because this upright microscope is originally designed for imaging thin, sectioned slices, and not for live animals. The trans-illumination unit (halogen lamp, condenser, sub-stage and turret) was removed entirely from the microscope, as confocal imaging never requires transmitted light, which allowed for more space between the microscope stage and the objective lens. The motorized stage was set as low as possible onto a customized framework, and a custom-designed height-adjustable mouse stage was fixed onto the motorized stage. Small temperature controller (Thermoplate; Tokai Hit Co., Ltd., Shizuoka, Japan) was integrated to the mouse stage [Fig. 1(a)]. For sample imaging, a custom-designed height adjustable coverslip holder is placed onto the tissue of interest to provide a flat surface for the objective lens [Fig. 1(b)]. The coverslip must be perpendicular to the objective lens, tightly fixed, and rigid enough so that the tissue of interest will not move during the imaging, but not so tight as to restrict blood flow. The detailed blueprint of the custom-designed mouse stage and the coverslip holder (fabricated and assembled by Sigma Koki Co. Ltd., Tokyo, Japan) will be provided upon request.

Fluorescent reagents

Hoechst 33342 dye (8 mg/kg in PBS, Lonza Group Ltd., Basel, Switzerland) was used to stain the nuclei of cells present in circulation and in the perivascular space. Evans Blue dye (8 mg/kg in PBS, Wako Pure Chemical Industries, Ltd., Osaka, Japan), which binds to plasma albumin, was used to stain the vasculature. Fluorescein (4 mg/kg in PBS, molecular weight of 332.31, Alcom Japan, Ltd., Tokyo, Japan) and fluorescein-labeled dextrans with average molecular weights of 10k, 70k, 500k (Invitrogen Corporation, Carlsbad, CA, USA) were used to study molecular weight-dependent pharmacokinetics. For the comparison study of normal and hydrodynamic injection, psFLT-1 plasmid DNA was labeled with Cy5 using Label IT Tracker Nucleic Acid Localization Kits (Mirus Bio Corporation, Madison, WI, USA).

Surgical procedures

All animal experimental procedures were executed in accordance with the Guide for the Care and Use of Laboratory Animals as stated by the National Institutes of Health. Mice were anesthetized with 2.0-3.0% isoflurane (Abbott Japan Co., Ltd., Tokyo, Japan) using a Univentor 400 Anaesthesia Unit (Univentor Ltd., Zejtun, Malta). Mice were then subjected to lateral tail vein catheterization with a 30-gauge needle (Becton, Dickinson and Co, Franklin Lakes, NJ, USA) connected to a non-toxic, medical grade polyethylene tube (Natsume Seisakusho Co., Ltd., Tokyo, Japan). Catheterization technique is described elsewhere (<http://imaging.bme.ucdavis.edu/surgical.html>). This catheterization allows multiple and timed injection without moving the mouse during data acquisition.

Ear lobe dermis tissue was accessible without surgery and easily fixed beneath the cover slip with a single drop of immersion oil. Tumor, kidney, or liver tissues were accessed following exteriorization through skin incision. For tumor imaging, female BALB/c nude mice were inoculated subcutaneously with H2B-GFP cells, which express green fluorescence protein in cell nuclei. Tumors were allowed to mature until the size of the tumor reached 5 mm in diameter. To minimize bleeding during the surgical procedure required to present tumors for imaging, a Surgitron (R) radio-frequency surgical device equipped with a Vari-Tip (TM) Wire Electrode (Cat. No. A8D) (Ellman International Inc., Oceanside, NY, USA) was used for bloodless, micro smooth incision with minimal tissue alteration.

Movie and time-lapse image acquisition

Video acquisition at a speed of 30 frames per second was performed for the indicated times, followed by time-lapse imaging every 1 minute. Drugs were administered via the tail vein catheter 10 seconds after video acquisition was initiated.

Acknowledgments

We thank Teru Kanda (Aichi Cancer Center Research Institute) for HeLa H2B-GFP cells. We thank Masabumi Shibuya (Tokyo Medical and Dental University) for providing pVL 1393 baculovirus vector pDNA encoding human sFLT-1. We thank Yoko Hasegawa, Mika Zenibayashi, Kotoe Date, Satomi Ogura, and Katsue Morii (The University of Tokyo) for technical assistance. T.O. is an employee of Nikon Instech Co., Ltd. All other authors declare no conflict of interest. This work was supported by Core Research Program for Evolutional Science and Technology (CREST) from the Japan Science and Technology Corporation (JST) (K.K.), Funding Program for World-Leading Innovative R&D on Science and Technology (FIRST Program) from Japan Society for the Promotion of Science (JSPS)(K.K.), and Grants-in-Aid for Scientific Research from the Japanese Ministry of Education, Culture, Sports, Science and Technology of Japan (21890051) (Y.M.).